2D Supramolecular Assemblies of Benzene-1,3,5-triyl-tribenzoic Acid: Temperature-Induced Phase Transformations and Hierarchical Organization with Macrocyclic Molecules

Mario Ruben,*,[†] Dietmar Payer,[‡,⊥] Aitor Landa,[†] Alessio Comisso,[§]
Chiara Gattinoni,[§] Nian Lin,*,[‡] Jean-Paul Collin,[||] Jean-Pierre Sauvage,[||]
Alessandro De Vita,[§] and Klaus Kern[‡,⊥]

Contribution from the Institut für Nanotechnologie, Forschungszentrum Karlsruhe GmbH, PF 3640, D-76021 Karlsruhe, Germany, Max-Planck-Institut für Festkörperforschung, Heisenbergstrasse 1, D-70569 Stuttgart, Germany, Physics Department, King's College London, Strand, London WC2R 2LS, U.K., CNR-INFM DEMOCRITOS National Simulation Center and Center of Excellence for Nanostructured Materials (CENMAT), University of Trieste, Italy, Laboratoire de Chimie Organo-Minérale, Université Louis Pasteur/U.M.R. du CNRS n° 7513, Institut Le Bel, 4, rue Blaise Pascal, 67070 Strasbourg-Cedex, France, and Institut de Physique des Nanostructures, Ecole Polytechnique Fédérale de Lausanne, 1015 Lausanne, Switzerland

Received May 23, 2006; E-mail: mario.ruben@int.fzk.de; n.lin@fkf.mpg.de

Abstract: Two-dimensional supramolecular honeycomb networks with cavities of an internal diameter of 2.95 nm were formed by the self-assembly of 4,4′,4″-benzene-1,3,5-triyl-tribenzoic acid (**BTA**) on a Ag-(111) surface at room temperature. Annealing to higher temperatures resulted in two sequential phase transformations into closer-packed supramolecular arrangements. The phase transformations are associated with stepwise deprotonation of the carboxylic acid groups. The voids of the honeycomb network of **BTA** have a suitable size for the construction of hierarchical structures with guest molecules. Single molecules of the macrocyclic compound **mt-33** were successfully confined inside 2D nanocavities of the honeycomb networks and released when the phase was transformed to the close-packed structure.

1. Introduction

The structures of materials follow a bottom-up scale change from the nano- to the macro-level with increasing structural and functional integration. The controlled fabrication, manipulation, and implementation of nanosized molecular entities into complex architectures have been intensively investigated, whereby the supramolecular self-assembly approach enables a high degree of molecule-directed structural organization within the nano-regime. Ideally, as realized in nature, reversible noncovalent bonds mediate the controlled assembly and hierarchical growth of instructed, fully integrated operational systems.[1]

Understanding how molecular entities self-arrange via non-covalent interactions is a key step for the realization of (supra)-molecular devices by bottom-up construction.[2] The control of the self-assembly of functionalized molecules in two-dimensions (2D) on solid surfaces may open the way to applications such as organic network templates, molecular electronic devices,[3a] or motors.[3b] The structure of organic monolayers on solid surfaces depends strongly on the size, function, and symmetry of both the molecular building blocks and the underlying substrate.[4] In addition, supramolecular assembly processes frequently involve structural phase transformations, in which the different structures exhibit only very small energy differences.[5] Understanding and controlling supramolecular structures becomes of fundamental importance for the design of nano-structured materials.

In particular, trimesic acid (TMA, $C_6H_3(COOH)_3$) represents a prototype system for the formation of 2D networks providing open voids. Studies dealing with scanning tunneling microscopy (STM) investigations of TMA and its derivatives on graphite (HOPG) or single-crystal noble metal surfaces have recently

† Institut für Nanotechnologie.
‡ Max-Planck-Institut für Festkörperforschung.
§ King's College London and CNR-INFM-DEMOCRITOS/CENMAT.
|| ULP/CNRS.
⊥ EPFL.

(1) Lehn, J.-M. *Science* **2002**, *295*, 2400−2403. Lehn, J.-M. *Proc. Natl. Acad. Sci. U.S.A.* **2002**, *99*, 4763. Ruben, M. *Angew. Chem., Int. Ed.* **2005**, *44*, 1594.
(2) Uosaki, K.; Yamada, R. *J. Am. Chem. Soc.* **1999**, *121*, 4090.

(3) (a) Lehn, J.-M. *Supramolecular Chemistry Concepts and Perspectives*; VCH: Weinheim, 1995. (b) Sauvage, J.-P. *Molecular Machines and Motors, Structure & Bonding, vol. 99*; Springer: Berlin, Heidelberg, 2001.
(4) (a) De Feyter, S.; De Schryver, F. C. *Chem. Soc. Rev.* **2003**, *32*, 139 and references therein. (b) Barth, J. V.; Costantini, G.; Kern, K. *Nature* **2005**, *437*, 671. (c) Barth, J. V.; Weckesser, J.; Cai, C.; Günter, P.; Bürgi, L.; Jeandupeux, O.; Kern, K. *Angew. Chem., Int. Ed.* **2000**, *39*, 1230. (d) Barth, J. V.; Weckesser, J.; Trimarchi, G.; Vladimirova, M.; De Vita, A.; Cai, C.; Brune, H.; Günter, P.; Kern, K. *J. Am. Chem. Soc.* **2002**, *124*, 7991.
(5) (a) Moulton, B.; Zaworotko, M. J. *Chem. Rev.* **2001**, *101*, 1629 and references therein. (b) Stepanow, S.; Lin, N.; Vidal, F.; Landa, A.; Ruben, M.; Barth, J. V.; Kern, K. *Nano Lett.* **2005**, *5*, 901.

Scheme 1. Molecular Structure of 4,4′,4″-Benzene-1,3,5-triyl-tribenzoic Acid (**BTA**)
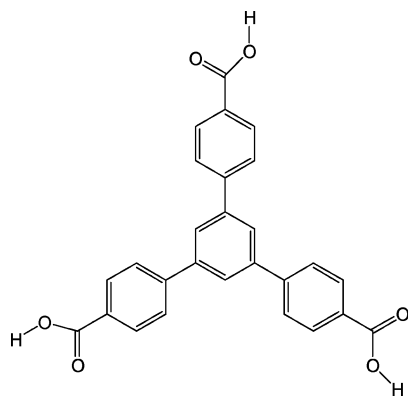
appeared.[6−12] Under vacuum conditions it was reported that TMA molecules adsorbed on HOPG form an open honeycomb structure,[6a] which can be modulated by the addition of long-chain alkanols.[6b] On Cu(100) and Ag(111) open honeycomb networks were also formed at temperatures below 280 K.[8,9] On Cu(100) the honeycomb phase is transformed into a striped array at room temperature (>300 K). As it may be expected, the planar adsorption geometry of the TMA molecules in honeycomb networks transforms into an upright geometry due to deprotonation of carboxylic functions at higher temperatures. Furthermore, it was found that under strong acidic conditions TMA also forms 2D networks on an Au(111) surface, which can be transformed into several phases by changes in the electric potential.[10,11] More recently, two different TMA-acid derivatives with flexible extensions were investigated on Ag(111) in HClO₄, exhibiting either open hexagonal or column-like networks depending on the molecular structure.[12]

Here, we report on the 2D self-assembly of a phenyl-extended version of TMA, the 4,4′,4″-benzene-1,3,5-triyl-tribenzoic acid (**BTA**), which was synthesized as described elsewhere.[13] The chemical structure of the **BTA** molecule is shown in Scheme 1: three 4′-benzoic acid groups are arranged around the central benzene core in a 3-fold symmetry. We find that **BTA** displays a more complex assembly behavior than its homologue TMA, involving three distinct supramolecular structures occurring at different temperatures on the Ag(111) surface. We have determined the supramolecular structures and the mechanics of the structural transformations by combined scanning tunneling microscopy (STM) measurements and theoretical modeling. In particular, our study demonstrates the important role that surface chemical reactivity plays in 2D supramolecular assembly. We

also demonstrate that one of the **BTA** supramolecular structures can include guest molecules forming a hierarchically organized molecular assembly.

2. Experimental Section

Synthesis. The syntheses of **BTA**[13] and **mt-33**[14] were carried out following literature procedures, and the obtained products were sublimed two times before use.

Sample Preparation. The sample preparation was carried out in an ultrahigh vacuum (UHV) system providing well-defined conditions for the experiment. The UHV system (base pressure ∼5 × 10⁻¹¹ mbar) is equipped with a home-built UHV-STM operating at 5 K. The atomically flat clean Ag(111) surface was prepared by several cycles of sputtering with argon ions and subsequent annealing at 850 K. **BTA** (in powder form) was deposited by organic molecular beam epitaxy (OMBE) from a Knudsen-cell evaporator with the temperature of the cell constantly held at 550 K during the evaporation. The macrocycle **mt-33** (in powder form) was deposited onto the **BTA** structured Ag(111) surface by OMBE with the crucible held at a temperature of 590 K. The Ag(111) substrate was maintained at a temperature of 300 K during deposition.

STM Measurements. The prepared sample was transferred to an STM stage in-situ without breaking the vacuum and cooled down to 5 K for data acquisition. The STM measurements were performed in the constant-current mode with electrochemically etched W-tips. Tunneling spectra were acquired by holding the STM tip at a constant height over the **BTA** molecules, and differential conductance spectra were recorded using a lock-in amplifier set to a frequency of 5 kHz and a modulation-amplitude of 10 mV. The cleanness of the tip was proved by obtaining typical surface state spectra at the clean Ag surface area before and after acquiring spectra on molecules. The spectra of the clean Ag were also used to normalize the spectra taken on molecules.

Computational Modeling. The structures revealed by the STM images were modeled by means of a combination of classical and ab initio molecular dynamics techniques. First-principles calculations were carried out using the Car−Parrinello method,[15] with Troullier Martins norm-conserving pseudopotentials[16] and a gradient corrected exchange-correlation functional.[17] The plane wave expansions were limited by a 50 Ry energy cutoff for gas-phase calculations, and the Brillouin zone sampling was limited to the gamma point only. For metallic systems, we introduced a 0.25 eV Fermi level smearing and raised the energy cutoff to 70 Ry. The classical constant-temperature simulations were performed using the AMBER package with the Generalized Amber Force Field and a Nose−Hoover thermostat. As the AMBER package does not allow direct modeling of metal surfaces, we modeled the metal substrate by a planar "carpet" of benzenes constrained to fixed positions. However, electrostatic interactions between the molecules and the metal surface are not taken into account by this approach.

To investigate this effect, we used a homemade 2D molecular dynamics model where surface screening effects are described by introducing mirror images of the force-field partial Coulomb charges[18] (ball and stick images are produced with Xcrysden[19] and VMD[20]).

3. Results and Discussion

STM Studies. The sublimation of the **BTA** molecules onto a Ag(111) surface held at 200−250 K followed by short

(6) (a) Griessl, S.; Lackinger, M.; Edelwirth, M.; Hietschold, M. *Single Mol.* **2002**, *3*, 25. (b) Nath, K. G.; Ivasenko, O.; Miwa, J. A.; Dung, H.; Wuest, J. D.; Nanci, A.; Perepichka, D. F.; Rosei, F. *J. Am. Chem. Soc.* **2006**, *128*, 4212.

(7) Lu, J.; Zeng, Q.; Wang, C.; Zheng, Q.; Wan, L.; Bai, C. *J. Mater. Chem.* **2002**, *12*, 2856.

(8) Dimitriev, A.; Lin, N.; Weckesser, J.; Barth, J. V.; Kern, K. *J. Phys. Chem. B* **2002**, *106*, 6907.

(9) Lin, N.; Payer, D.; Dmitriev, A.; Strunskus, T.; Wöll, C.; Barth, J. V.; Kern, K. *Angew. Chem., Int. Ed.* **2005**, *44*, 1488.

(10) Ishikawa, Y.; Ohira, A.; Sakata, M.; Hirayama, C.; Kunitake, M. *Chem. Commun.* **2002**, 2652.

(11) Su, G.-J.; Zhang, H.-M.; Wan, L.-J.; Bai, C.-L.; Wandlowski, T. *J. Phys. Chem. B* **2004**, *108*, 1931.

(12) Yan, H.-J.; Lu, J.; Wan, L.-J.; Bai, C.-L. *J. Phys. Chem. B* **2004**, *108*, 11251.

(13) Schwab, P. F.; Fleischer, F.; Michl, J. *J. Org. Chem.* **2002**, *67*, 443.

(14) Livoreil, A. L.; Dietrich-Buchecker, C. O.; Sauvage, J.-P. *J. Am. Chem. Soc.* **1994**, *116*, 9399.

(15) Car, R.; Parrinello, M. *Phys. Rev. Lett.* **1985**, *55*, 2471.

(16) Troullier, N.; Martins, J. L. *Phys. Rev. B* **1991**, *43*, 1993.

(17) Perdew, J. P.; Wang, Y. *Phys. Rev. B* **1992**, *45*, 13244.

(18) Vladimirova, M.; Stengel, M.; De Vita, A.; Baldereschi, A.; Boeringer, M.; Morgenstern, K.; Berndt, R.; Schneider, W. D. *Europhys. Lett.* **2001**, *56*, 254.

(19) Kokalj, A. *Comput. Mater. Sci.* **2003**, *28*, 155.

(20) Visual Molecular Dynamics: http://www.ks.uiuc.edu/Research/vmd/.

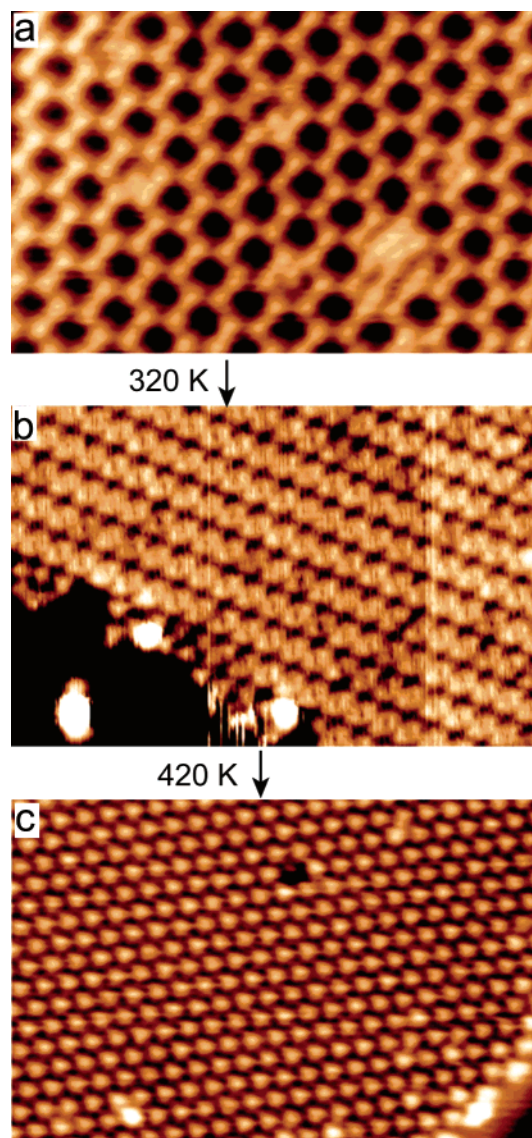**Figure 1.** The deposition of the **BTA** molecules onto a Ag(111) surface results in the formation of three different supramolecular hydrogen-bonding motifs depending on the Ag(111) surface temperature: (a) phase I (open 2D honeycomb network), (b) phase II (1D ribbons), and (c) phase III (close-packed 2D adlayer). Image size: 30 nm × 20 nm. Tunneling current = 0.5 nA, bias voltage = 0.5 V (applied to the sample).

annealing at 270−300 K resulted in the formation of a regular 2D honeycomb network (Figure 1a). However, holding the temperature of the Ag(111) surface above 320 K during the molecular deposition resulted in the evolution of a second phase of ribbons consisting of equal-spaced one-dimensional (1D) rows (Figure 1b). Alternatively, phase I (the 2D open honeycomb network) can be transformed into phase II (the 1D ribbon structure) by annealing at a temperature of 320 K. Further increasing the temperature of the Ag(111) surface above 420 K resulted in the emergence of a phase III, in which a 2D close-packed adlayer with inherent 3-fold symmetry could be observed (Figure 1c). All three phases are formed in extended domains on the surface. Both phase transformations were completely irreversible.

To investigate the origin of the phase transformations, tunneling spectra were acquired at the three phases. The electronic structure of an adsorbed molecule is perturbed by
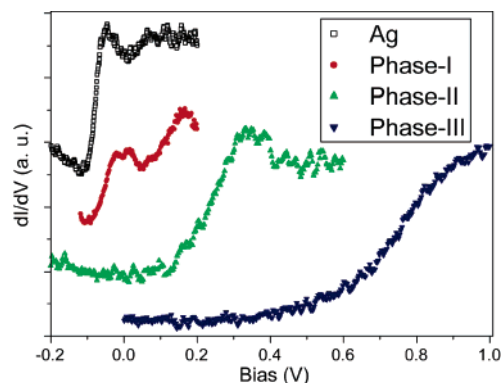

Figure 2. dI/dV tunneling spectra acquired at the three phases, respectively. As a reference, the spectrum acquired at the pristine Ag(111) surface is shown, displaying the surface state onset at −70 mV. All spectra were taken at 5 K in lock-in technique, with a modulation amplitude of 10 mV and a modulation frequency of 5 kHz. Setting parameters of measurements (tunneling current and bias voltage before opening the feedback loop) are 0.2 V and 1.5 nA, 0.2 V and 0.7 nA, 0.6 V and 0.5 nA, and 1.0 V and 1.0 nA, for acquiring spectra on clean Ag, phase I, phase II, and phase III, respectively. The magnitude of each spectrum is normalized according to the onset height of the clean Ag surface state taken with the same setting parameters. The curves are shifted along the Y-axis for clarity.

the presence of the substrate electrons, and vice versa.[21] For weak adsorbate−substrate interaction, the Shockley surface state present on the (111) surfaces of the noble metals Au, Ag, and Cu is known to persist upon adsorption with modified band onset and electron/hole lifetimes.[22,23] An excess negative charge at the surface associated with the adsorption usually results in an upward shift of the onset energy,[22b−d] whereas a downward shift is observed for electron-deficient adsorbates such as alkali metals.[23] Stronger adsorbate−substrate interactions can lead to substantial changes of the substrate electronic structure and even quenching of the surface state. Figure 2 shows the dI/dV tunneling spectra of the three molecular phases along with the clean Ag(111) spectrum. The latter shows a sharp onset at −70 mV. This steplike characteristic is modified by the adsorption of **BTA** in all three phases. In phase I, a slightly broader onset at energy of −50 mV was observed (the onset position is defined by the half-maximum height). In contrast, phase II and phase III show onsets of remarkable broadening and upward shifting, 320 and 770 mV, respectively. The spectra are independent of the position of the STM tip; that is, scanning tunneling spectroscopy (STS) mapping of **BTA** at various essential energies does not display submolecular contrast. This phenomenon suggests that the observed spectral features are not derived from **BTA** molecular orbitals,[24] but rather from the Ag surface electronic states.

Phase I consists of neutral **BTA** that weakly adsorbs at the surface, which only slightly alters the surface state onset.[22a] The significant upward shift in phase II and III indicates the presence

(21) (a) Zou, Y.; Kilian, L.; Schöll, A.; Schmidt, C.; Fink, R.; Umbach, E. *Surf. Sci.* **2006**, *600*, 1240−1251. (b) Eremtchenko, M.; Schaefer, J. A.; Tauz, F. S. *Nature* **2003**, *425*, 602.
(22) (a) Hovel, H.; Grimm, B.; Reihl, B. *Surf. Sci.* **2001**, *477*, 43. (b) Paniago, R.; Matzdorf, R.; Meister, G.; Goldmann, A. *Surf. Sci.* **1995**, *325*, 336. (c) Jacob, W.; Dose, V.; Goldmann, A. *Appl. Phys. A* **1986**, *41*, 145. (d) Lindgren, S. A.; Paul, J.; Wallden, L. *Surf. Sci.* **1982**, *117*, 426. (e) Chen, C. T.; Smith, N. V. *Phys. Rev. B* **1989**, *40*, 7487.
(23) (a) Lindgren, S. A.; Wallden, L. *Solid State Commun.* **1980**, *34*, 671. (b) Lindgren, S. A.; Wallden, L. *Phys. Rev. Lett.* **1987**, *59*, 3003.
(24) (a) Sautet, P.; Bocquet, M.-L. *Phys. Rev. B* **1996**, *53*, 4910. (b) Repp, J.; Meyer, G. *Phys. Rev. Lett.* **2005**, *94*, 026803. (c) Kraft, A.; Temirov, R.; Henze, S. K. M.; Soubatch, S.; Rohlfing, M.; Tautz, F. S. *Phys. Rev. B* **2006**, *74*, 041402.
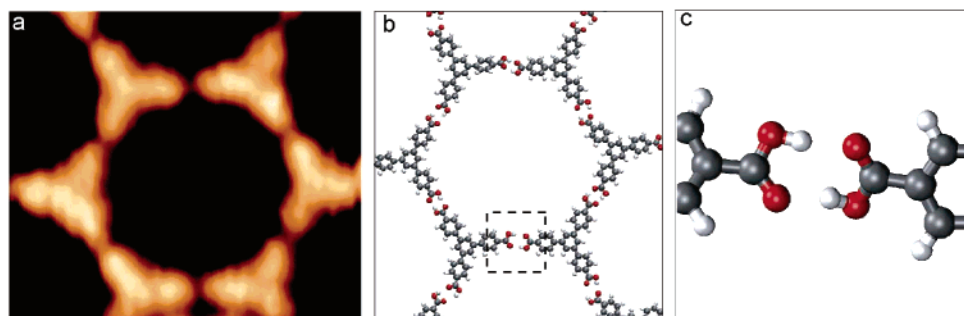
Figure 3. (a) High-resolution STM image of the phase I honeycomb network. Image size: 4.9 nm × 4.3 nm. (b) Atomistic model proposed for this phase. (c) The modeled double hydrogen bond between two carboxylic acid groups. Tunneling current = 0.5 nA, bias voltage = 0.5 V (applied to the sample).
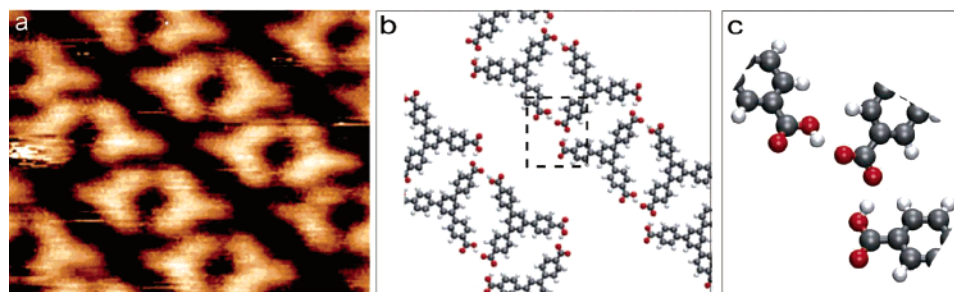

Figure 4. (a) High-resolution STM image of the phase II ribbon structure. Image size: 6.1 nm × 4.7 nm. (b) Atomistic model obtained for this chiral asymmetric structure. Each molecule is singly deprotonated, but still links to neighboring molecules by hydrogen bonds between carboxylic acid pairs. (c) Detail of the hydrogen-bond corner linkage. Tunneling current = 0.5 nA, bias voltage = 0.5 V (applied to the sample).

of negatively charged adsorbates at the surface, which is associated with deprotonated acid groups. This observation is consistent with recent experiments on the related molecule trimesic acid on Ag(111), where deprotonation of the carboxylic acid groups also resulted in an upward shift (330 mV) of the surface state onset.[25] The further shifting and broadening of the onset of phase III with respect to phase II reflects (and is possibly caused by) the development of the deprotonation processes, that is, a stepwise increase of the number of deprotonated groups per **BTA** molecule,[23b] consistent with the irreversibility of the observed transitions.

On the basis of these observations, we propose the following models for the three **BTA** phases. Phase I represents a 2D open hexagonal network, which incorporates a regular array of cavities of 2.9 nm inner diameter and 3.1 nm periodicity (Figure 3a). The supramolecular interconnection of the **BTA** molecules is achieved by symmetric hydrogen bonds of carboxylic acid dimers, as shown in Figure 3b and c, whereby the oxygen−oxygen distance is estimated at a value of 3.1 Å, as expected for this type of bond. Structurally, the honeycomb phase I is similar to that of the related TMA systems, although the pore size is significantly enlarged to 2.95 nm.[5,8,9,26] Very recently, the same hexagonal network structure of the unprotonated **BTA** was also found at the solid/liquid interface (graphite/nonanoic acid or 1-phenyl octane).[27] Generally, two types of point defects can be observed: (i) missing bricks (BTA molecules) within

the hexagonal network and (ii) additional **BTA** molecules within the cavities (cf., Figure 1a). The latter defect suggests the possibility to achieve a controlled filling of the relatively large hexagonal cavities with different types of molecules.

Phase II has a 1D ribbon structure, as shown in Figure 4a. Within the single rows, two **BTA** molecules are arranged in pairs forming a band of 1.70 nm width. The periodicity along the row is 1.55 nm, and the row-to-row spacing is 2.18 nm. The orientations of the ribbons fall in three directions with a 120° angle in between, reflecting the 3-fold symmetry of the Ag(111) substrate. The structure of phase III consists of close-packed **BTA**, with every end group pointing to the mid-edge of an adjacent molecule, as shown in Figure 5a. This phase has a C_3 symmetry and a 1.36 nm lattice constant.

Computational Modeling. To investigate its stability, phase I was modeled with AMBER holding the system in a planar geometry. The resulting equilibrium structure is shown in Figure 3b. Although the benzene's surface model is probably less effective than on the real metal substrate in stabilizing the structure, the network proved to be stable up to relatively high temperatures in the modeling. The structure consists of a network of molecules doubly bound to each other by hydrogen bonds of the carboxylic acid groups (Figure 3c) to form a honeycomb network structure.

The ribbon phase II is far less immediate to model, as it presents molecules arranged in stripes that keep apart from each other (see Figure 4a). The AMBER package was next used to investigate the stability of the observed phase II ribbon structure. The simulations were carried out for different ribbon configurations imposing the same initial temperature, spacing, and substrate conditions. The rows were made of **BTA** molecules with the carboxylic acid groups either fully protonated or singly

(25) Payer, D.; Comisso, A.; Dmitriev, A.; Strunskus, T.; Lin, N.; Wöll, C.; De Vita, A.; Barth, J. V.; Kern, K., submitted.
(26) (a) Theobald, J. A.; Oxtoby, N. S.; Philips, M. A.; Champness, N. R.; Beton, P. H. *Nature* **2003**, *424*, 1029. (b) Stöhr, M.; Wahl, M.; Galka, C. H.; Riehm, T.; Jung, T. A.; Gade, L. H. *Angew. Chem., Int. Ed.* **2005**, *44*, 7394.
(27) Kampschulte, L.; Lackinger, M.; Maier, A.-K.; Kishore, R. S. K.; Griessl, S.; Schmittel, M.; Heckel, W. M. *J. Phys. Chem. B* **2006**, *110*, 10829.
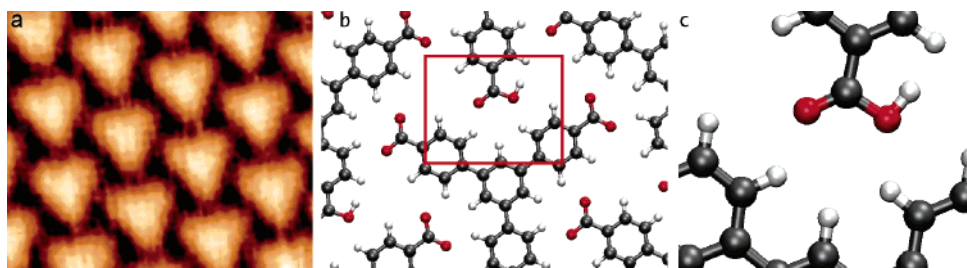
Figure 5. (a) High-resolution STM image of the phase III closely packed 2D adlayer structure. Image size: 5.6 nm × 4.4 nm. (b) Atomistic model of phase III. The **BTA** molecules are doubly deprotonated in this model (the remaining proton is tilted backward) with no residual H-bonds between carboxyl groups. (c) Hydrogen bonds between one remaining protonated carboxylic acid group and the C−H protons of the phenyl rings of neighboring **BTA** molecules. Tunneling current = 0.5 nA, bias voltage = 0.5 V (applied to the sample).

deprotonated. It was found that in both cases the rows appear to be stable up to high temperatures (500−600 K in the simulations). However, neighboring rows made of fully protonated molecules tend to stick to each other, contrary to what was observed in the STM images. On the other hand, when partially deprotonated molecules are used, neighboring parallel rows remain apart from each other during the simulations, consistent with the experimental results. These results were obtained again using the molecular dynamics model described in the Experimental Section, which contains an image-charge description of the surface screening. This all suggests that the observed behavior is due to the repulsive interaction between the neighboring rows containing negatively charged carboxylate groups on their borders. This electrostatic repulsion cannot be overcome by hydrogen bonds between carboxyl groups of neighboring chains, because all of the available carboxyl hydrogens are involved in the internal linkage structure of the individual chains. Furthermore, the repulsion can be expected to be significant at short intermolecular distances even after taking into account the surface electrostatic screening, yielding stable structures with separated molecular ribbons at the experimental coverages. The most stable molecular structure identified for phase II is the one shown in Figure 4b. It contains one deprotonated carboxylic acid group bound to two different protonated acid groups by two hydrogen bonds (Figure 4c). One of the hydrogen bonds is tilted backward, yielding a chiral stepped structure for the assembled row. This structure was found to be more stable than any other structure we could produce with further modeling. Also, it is the structure in best agreement with the observed images.

We note that while the honeycomb phase (phase I) corresponds to the optimal hydrogen-bonding geometry between fully protonated molecules, it would become relatively unstable if one carboxylic acid group per **BTA** were deprotonated, as this would imply couples of adjacent negatively charged mutually repelling oxygen atoms, located on the non-hydrogen-bonded side of facing carboxylic acid group pairs. We thus conclude that the observed phase II, which does not involve symmetric pairs of repulsive oxygens, would become more stable if deprotonation occurred. Although the lowered degree of direct carboxyl pairing does not taken alone prove that deprotonation occurs, we note that the onset of deprotonation, which is known to occur in similar systems and temperature range,[25] would be consistent with the tunneling spectra data and with the irreversibility of the observed transition. We thus suggest that thermally initiated deprotonation of the carboxylic acid groups is the driving force for the transition from phase I to phase II.

When further deprotonation takes place at higher temperatures ($T > 420$ K), as suggested by the tunneling spectrum taken at phase III, even the phase II ribbon configuration becomes unstable, because at least two hydrogens are needed to bind together three carboxylic acid groups. Experimentally, the system changes into the 2D close-packed phase III upon further annealing, with all **BTA** molecules having the same orientation. This third phase does not contain hydrogen bonds between carboxylic acid groups, and the molecules stabilize in a triangular 2D lattice (see Figure 5a), in which every end group points to the mid-edge of an adjacent molecule. At first, it would seem reasonable to assume that complete deprotonation of the carboxylic acid groups were implied by such a structure. However, classical modeling carried out with the same MD packages used above indicates that the high density of negative charges left by complete deprotonation introduces an exceedingly large repulsive contribution to the cohesive energy of the supramolecular structure. Indeed, any attempt to reproduce a stable packed structure of fully deprotonated ($-3e$ charged) molecular ions with classical codes failed, the repulsive energy term being too high for the system to remain stable. A simple estimate of the Coulomb repulsion energy can be obtained by approximating each negative carboxylic group (screened by the metal surface) with a standing electric dipole. The system thus becomes a network of dipoles set on a regular triangular lattice, with a repulsive energy per molecule of ∼10 eV. This should be compared to the attractive interaction between molecules, which can be estimated by ab initio modeling of the bonding of a deprotonated benzoic acid with one **BTA** molecule in the gas phase. In equilibrium the molecules are coplanar and bound by hydrogen bonds involving COO oxygens and CH group hydrogens. The distance between the carbons and the oxygens is approximately 2.95 Å, the geometry being similar to that of the hydrogen bonds formed by the two **BTA** COO-groups of the central molecule in Figure 5b. This calculation yields a binding energy of 1.8 eV per molecule, that is, much less than the repulsive contribution above. These results indicate that a fully deprotonated, fully charged system is unlikely to form, so that different states of charge or less than full deprotonation must be considered.

We thus modeled the fully deprotonated system with an ab initio simulation containing a single **BTA** molecule over 5 layers of Ag(111) in each periodically repeated cell of a triangular surface lattice. After electronic and ionic relaxation, the electron density was integrated over the volume occupied by the molecule to evaluate its charge state. Our calculated value for the charge of the fully deprotonated adsorbed molecule is
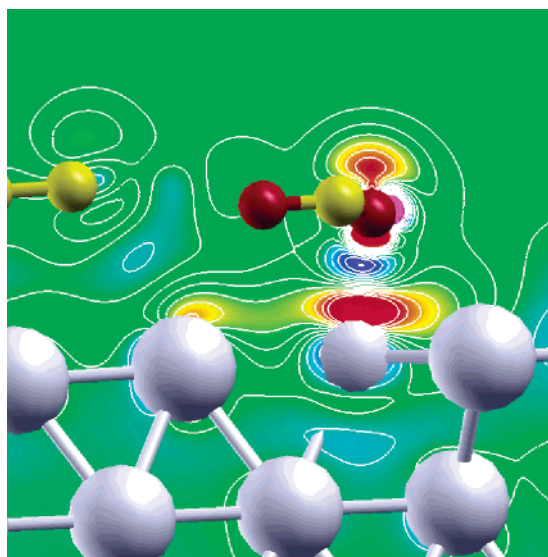
Figure 6. Contour plot of the electron density displacement in a vertical plane containing an oxygen belonging to a deprotonated carboxylate group (see text). Electron density depletion is plotted in red-yellow, while the blue-green color palette denotes electron density accumulation.

$-1.97e$; that is, the model predicts that the molecule is less negatively charged than the previously considered $-3e$ value. The repulsive energy estimated as before decreases to ∼4.5 eV in this case, which is still too high to yield the close-packed configuration of phase III.

We then addressed the alternative hypothesis of incomplete deprotonation, implying, for example, that a doubly deprotonated system should be compatible with the geometry of the system. An ab initio calculation revealed that the phase III arrangement is still compatible with the presence of protonated oxygens if the OH bond is tilted backward. In such a system (see Figure 5b), the calculated ab initio value for the integrated charge of the molecule is $-1.17e$, corresponding to an estimated repulsive energy of ∼1.5 eV, which is low enough to be compatible with the occurrence of a close-packed stable structure in which carboxyl groups are not facing each other. Thus, phase III is rationalized by a structure containing doubly deprotonated **BTA** molecules. In this phase, both the two deprotonated carboxylate groups and the still protonated carboxylic acid group bind to the inner pocket of aromatic C−H protons of the neighboring **BTA**, leading to an intermolecular hydrogen-bonding network, as shown in Figure 5b.

In the equilibrium configuration the molecules lay flat on the surface, at a distance of about 3.1 Å from the first Ag layer. The oxygens in the deprotonated group are slightly tilted toward the surface. The main feature of the electronic structure of the phase III monolayer is the dipolar layer corresponding to the overall $-1.17e$ charged molecule, screened by the metal surface. As discussed above, the main effect of the presence of the surface in mediating the interaction between deprotonated molecules is to define the long-range component of such interaction as the lateral repulsion between negative standing dipoles. To analyze the substrate−adsorbate interaction beyond dipole formation, we computed the displaced electron density on a vertical plane passing by an oxygen atom of a deprotonated carboxylate group (contour plot in Figure 6). To obtain this quantity, we first compute the electron density of the phase III

Scheme 2. Hierarchical Self-Assembly and Temperature-Controlled Release
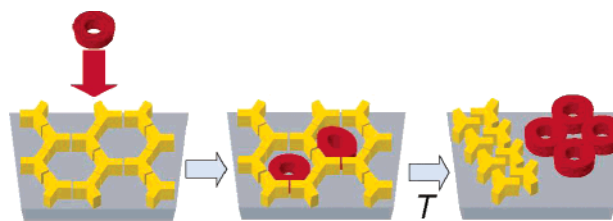
system. From this we subtract the electron densities associated to a gas phase $-e$ charged deprotonated molecule and that associated to the $+e$ surface unit cell, still assuming the phase III periodicity. As our choice of subtracted electron densities already approximately reproduces the final dipole structure of the interacting system (where the molecule is $-1.17e$ charged and the surface is $+1.17e$ charged), the displaced electron density as defined can be used to describe the further local density rearrangement occurring on the molecule and on the surface once the interaction between the two is turned on. The polarization of the oxygen atom in the negatively charged COO group and the screening response of the surface are visible in Figure 6 as a peak-through structure with a prominent electron accumulation lobe (in blue) located just below the oxygen atom. This is screened by a corresponding depletion lobe (in red) located just above the Ag surface layer. No similar structure is found for protonated (neutral) carboxyl groups, and no appreciable structure is detected plotting the electron density displacement in the horizontal plane of the BTA adlayer, suggesting that the metal substrate does not significantly modify the electronic structure of the H-bonding regions.

Hierarchical Self-Assembly. The bottom-up generation of organizational levels of increasing complexity, diversity, and functionality relies on hierarchic self-assembly steps, where each step progressively sets the base for the next one.[1,26] The nanocavities of the phase I honeycomb structure with 2.95 nm inner-diameter provide the space to bind a single molecule or a discrete number of guest molecules.[28] Because of its regular arrangement of nanocavities over extended domains, the supramolecular phase I structure constitutes an ideal two-dimensional template to construct an ordered hierarchical system with guest molecules. Furthermore, the temperature-controlled phase transformation leads to a reorganization under release of the guest molecules. These concepts are illustrated in Scheme 2.

To test the possibility of hierarchical self-assembly, molecules of the macrocylic compound **mt-33** (see Supporting Information Figure S1) were chosen as guest molecules. **mt-33** was deposited on top of the surface covered with the hexagonal 2D network of phase I. We found that single molecules of **mt-33** were confined within the nanometer-sized cavities of the hexagonal network. STM measurements, as shown in Figure 7, which were taken at 5 K, clearly identified larger species trapped in the honeycomb cavities, as represented by the red rings in the schematic graph of Figure 7b. The appearance of these objects occurred exclusively after the deposition of **mt-33**. The external size and the ellipsoidal shape indicate that these objects are indeed molecules of **mt-33** (see Supporting Information). In

(28) (a) Stepanow, S.; Lingenfelder, M.; Dmitriev, A.; Spillmann, H.; Delvigne, E.; Lin, N.; Deng, X.; Cai, C.; Barth, J. V.; Kern, K. *Nat. Mater.* **2004**, *3*, 229. (b) Stepanow, S.; Lin, N.; Barth, J. V.; Kern, K. *Chem. Commun.* **2006**, 2153.
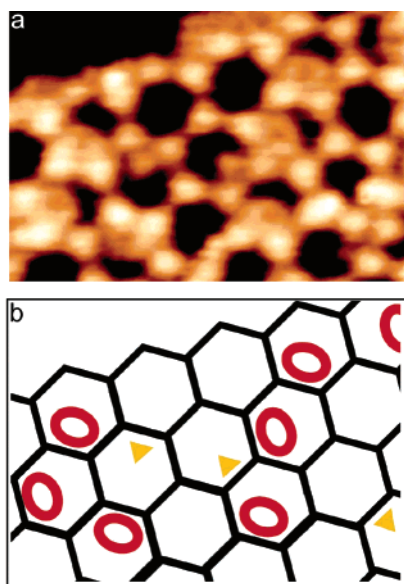
Figure 7. Trapping of single macrocycle molecules **mt-33** in the nano-cavities of phase I of **BTA**. (a) STM image (18 nm × 11 nm) representing the hexagonal network of **BTA** with subsequently deposited **mt-33**. (b) A schematic view of (a). The solid hexagons highlight the backbone of the honeycomb network, whereas the red rings show a single macrocycle molecule of **mt-33** trapped within cavities and the yellow triangles show trapped molecules of **BTA**. Tunneling current = 0.5 nA, bias voltage = 0.5 V (applied to the sample).

addition, the trapped molecules within the cavities exhibit a donut shape, which advocates for a flat adsorption on the surface. In comparison, the included smaller species (expressed as yellow triangles in the schematic view) are excess molecules of **BTA** trapped within cavities, which can be easily distinguished from the macrocyclic compound **mt-33**.

Figure 7a further reveals that due to the matching interior size of the cavity with the molecular size of **mt-33** only single species are accommodated in a cavity at these particular deposition conditions. In any case, no double inclusion of **mt-33** could be observed. In more detail, the STM data also reveal that the molecules are confined eccentrically within the hexagonal cavities contacting the cavity inner wall, which might be explained by the attractive interaction between the macrocycle outer rim and the cavity inner wall. The preference of the adsorption sites also reflects the stereochemical misfit of a C_2-symmetry molecule **mt-33** within a 3-fold-symmetric environment.

When annealing the phase I structure that included the trapped **mt-33** species to the phase transformation temperature of 320 K, the trapped **mt-33** molecules were released and formed dimers, trimers, and tetramers together with the close-packed phase II of **BTA**, as shown in Figure 8a. The individual molecule appears as a doughnut-shaped object, which reflects the ring structure of **mt-33**. The high-resolution data in Figure 8b and c elucidate an asymmetrically ellipsoidal shape of individual molecules of **mt-33** consisting of a broader 2,2′,6′,2″-terpyridine (denoted as head) part and a sharper 1,10-phenanthroline part (denoted as tail). Within the aggregates, the molecules form head-to-head arrangements for both the dimer and the tetramer. The intermolecular interactions are attributed to hydrogen bonds between the nitrogen atoms and the protons of the aromatic rings of all-transoid conformers of neighbored
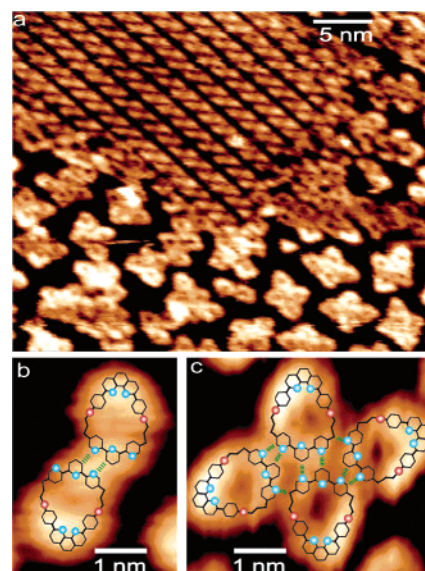

Figure 8. (a) STM image showing spontaneous clustering of macrocycle molecule **mt-33** coexisting with the close-packed phase II of BTA. (b and c) High-resolution STM images of the dimeric and tetrameric aggregates with inscribed models (nitrogen in blue; oxygen in red) and intermolecular hydrogen bond (in green). Tunneling current = 0.5 nA, bias voltage = 0.5 V (applied to the sample).

2,2′,6′,2″-terpyridine units, as proposed by the green dashed lines in Figure 8b and c. This nucleation behavior is identical to adsorption of **mt-33** at a clean Ag(111) surface (see Supporting Information Figure S2).

4. Conclusion

A 2D open honeycomb network with nanopores of an internal diameter of 2.95 nm was formed by the self-assembly of 4,4′,4″-benzene-1,3,5-triyl-tribenzoic acid (**BTA**) on Ag(111) surfaces. Stepwise annealing of the initial phase resulted in two phase changes: the 1D ribbon phase II and the 2D close-packed adlayer phase III. The tunneling spectra acquired at the three phases suggested that the phase transformations are due to progressive deprotonation of the carboxylic acid functions of **BTA**, in agreement with the irreversible transformation. Theoretical modeling by classical force fields and ab initio calculations has been used to reproduce and interpret the experimental results. The emerging physical picture is that whenone carboxylic acid group is deprotonated per **BTA** molecule, repulsion between facing carboxylic acid groups occurs and the first transition (phase I to phase II) takes place. If further deprotonation occurs, the intermolecular links within phase II, consisting of H-bonds between carboxyl acid groups, are progressively broken, and the second transition occurs. During these processes, stable hydrogen bonds connecting fully protonated opposite-facing carboxyl acid groups (phase I) are progressively substituted with lateral hydrogen bonds between partially deprotonated carboxyl acid groups (phase II) and finally by hydrogen bonds between carboxylic acid groups/carboxylates and phenyl C−H protons (phase III). In summary, our results indicate that deprotonation can explain the occurrence of the self-assembled phases in the observed order. Rather remarkably, they also exemplify how higher-coverage phases can be obtained at each step of a series of phase transitions in

a supramolecular assembled system, despite the increasing temperature and the increasing electrostatic energy cost accompanying deprotonation.

The voids of the honeycomb network **BTA** have a suitable size for the construction of hierarchical structures with guest molecules. Single molecules of the macrocyclic compound **mt-33** were successfully confined inside 2D nanocavities of phase I and released when the phase transformed to the close-packed structure, forming dimeric and tetrameric clusters. Further investigations of the use of these large open cavities as quantum resonators, nanoreactors for chemical reactions, or as templates

for single-molecule addressing of appropriate guests are underway.

Supporting Information Available: Single-crystal X-ray structure of **mt-33** (S1), and STM images of clusters of **mt-33** on Ag(111) (S2). This material is available free of charge via the Internet at http://pubs.acs.org.

JA063601K